Internal Flow Visualization of a Large-Scaled VCO Diesel Nozzle with Eccentric Needle

T. Oda[1*], K. Ohnishi[1], Y. Gohda[2], T. Sumi[1] and K. Ohsawa[1]
[1] Department of Mechanical Engineering, Tottori University, Japan
odate@mech.tottori-u.ac.jp, kenichifuji@gmail.com,
sumi@mech.tottori-u.ac.jp, ohsawa@mech.tottori-u.ac.jp
[2] Mitsubishi Material Techno Co., Japan
kzhr.55344.mp4-20@ezweb.ne.jp

Abstract

Flow visualization was performed to investigate the effects of eccentricity of a needle inside a valve-covered-orifice (VCO) diesel nozzle on structure of internal flow. A 10 times large-scaled VCO nozzle with two holes was employed for visualization. The needle, which was incorporated into the nozzle, was manipulated by a three-dimensional traverse with micrometers. Discussion in this study focuses on the behavior observed at relatively low needle lift, and the needle is manipulated vertical to both the holes. Flow visualization for first mode of internal flow, which leads to the solid cone spray, indicates almost straight stream with weak swirl motion and with contraction regions at the upper side and lower side of the entrance when the eccentric needle is located close to the nozzle center. On the other hand, the second mode of internal flow is encountered when the distance of the needle from the nozzle center is further increased beyond the location of the first mode. The flow pattern of the second mode shows strong swirl motion, which mainly produces the hollow cone spray, and exhibits a upperside contraction region at the hole entrance although the lowerside contraction region at the hole entrance becomes undetectable. The swirl motion and the contraction region affect the behavior of the primary breakup.

Introduction

The valve-covered-orifice (VCO) nozzles are usually employed in order to reduce unburned hydrocarbon emissions. However some researchers [1,2,3,4] have qualitatively revealed that different size sprays were emerged from real-size VCO nozzles because of radially eccentric locations of needles incorporated into the nozzles. As a result, asymmetric combustion and soot formation are yielded in diesel engines [1].

The large-scaled transparent nozzles have been used frequently, so that cavitating bubbles and resulting sprays could have been easily observed [5,6]. At very low needle lifts string-like bubbles, so called the vortex cavitating bubbles, and hollow cone sprays have been observed. We performed a steady-state experiment byusing a 10 times large-scaled VCO nozzle with good spatial resolution of a 3-D traverse to manipulate a needle due to obtaining quantitative information [7,8]. The experimental result shows that the cavitating bubbles and the resulting sprays were very sensitive to the radially eccentric locations of needles. Especially, manipulation of the needle vertical to a nozzle hole caused complicated behavior of the bubbles and the sprays. In addition to the experimental study, a three-dimensional computational fluid dynamic (CFD) simulation of cavitating flows by employing the simplified Rayleigh's model for cavitation and the Volume of Fluid (VOF) model for an air-core inside nozzle hole was performed [9,10]. This numerical study seems to imply that axial momentum and angular momentum of internal flow might play an important role in the flow pattern inside the hole.

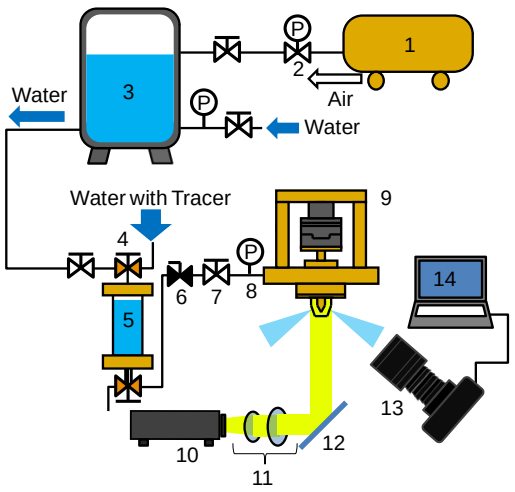

1. Compressor 2. Regulator 3. Accumulator 4. 3Way Valve
5. Tracer Mixing Chamber 6. Needle Valve 7. Ball Valve
8. Pressure Gauge 9. Nozzle Holder and Test Nozzle
10. Slide Projector 11. Lens 12. Mirror 13. Digital Camera 14. PC

Figure 1 Schematic of a injection system.

* Corresponding author: odate@mech.tottori-u.ac.jp

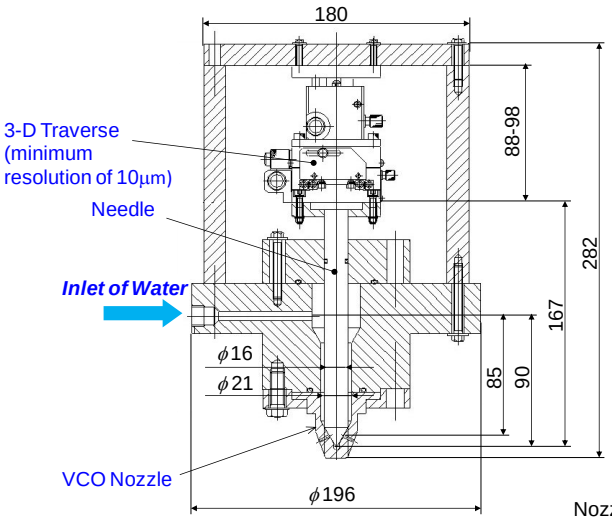

Figure 2 Schematic of nozzle holder with 10 times large-scaled VCO nozzle.

In this paper we present experimental results of flow visualization inside the large-scaled transparent VCO nozzle by using fine tracer particles. Our discussion mainly focuses on the behaviors at relatively low needle lift, and the needle is manipulated vertical to a nozzle hole. Thus the flow patterns obtained are compared with behaviors of the cavitating bubbles and the primary atomization.

Experimental Procedure

Figure 1 shows a schematic of an experimental setup for the present study. An accumulator containing water, which was employed as the test liquid, was pressurized by an air compressor up to 1.2MPa. A pressure regulator was used to maintain the pressure in the accumulator. The water from the accumulator passed steadily through a needle valve and a Bourdon-type pressure gauge, which were used to control the injection pressure, before the water attained a nozzle holder. A ball valve, which was located between the needle valve and the Bourdon-type pressure gauge, and a tracer mixing chamber, which was located between the accumulator and the needle valve, were not used when spark photographs of cavitating bubbles inside a large-scaled VCO nozzle and sprays were taken. However the ball valve and the tracer mixing chamber were used for flow visualization inside the nozzle. Flow rate of water without tracer particles was set in terms of the pressure gauge reading by using the needle valve before the flow visualization, and then the ball valve was closed to put water with the tracer particles into the tracer mixing chamber. Finally, the ball valve was opened, so that the water inside the tracer mixing chamber, which was pressurized by

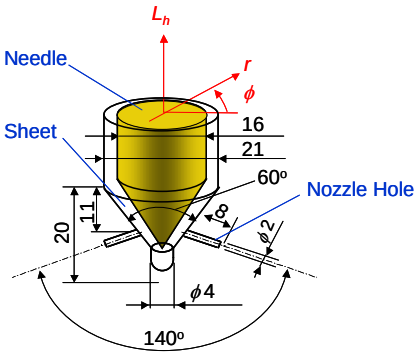

(a) Nozzle geometry and coordinate system

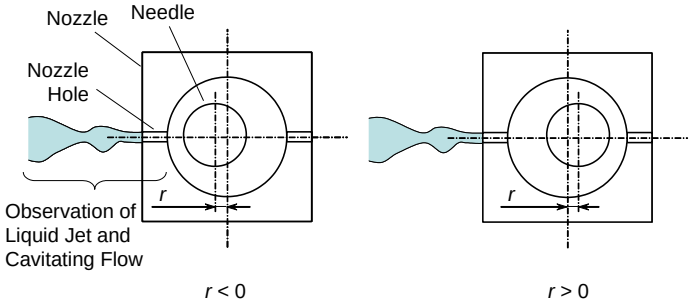

(b) Radial location of needle at azimuthal angle of 0°

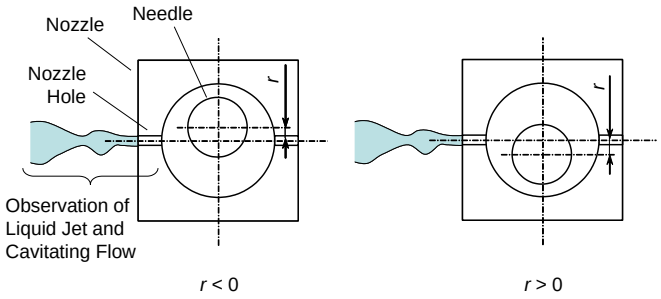

(c) Radial location of needle at azimuthal angle of 90°

Figure 3 Schematic of nozzle geometry and coordinate system.

Table 1 Specifications of tracer particles for flow visualization.

Tracer Particles	Cross-Linked Poly (Methyl Methacrylate)
Density	1.20 kg/m^3
Diameter	50 μm
Concentration of Particles	1.6 mg/cc-water
Surfactant	Poly Oxyethylene Alkyl Ether
Concentration of Surfactant	0.05 g/cc-water

the water in the accumulator, was supplied into the nozzle holder, and the water was ejected from nozzle holes to the quiescent atmospheric air.

Figure 2 illustrates the nozzle holder. The water was introduced into an inlet of the nozzle holder before flowing a pre-nozzle region which was located just upstream of a seat. A needle was incorporated into the nozzle holder, and had a diameter of 16mm and a 60°-edge tip. A large-scaled VCO nozzle, which was made of transparent acrylic resin, was mounted underneath the nozzle holder. The needle was mounted underneath the 3-D traverse with three micrometers which could provide a minimum resolution of 10μm. The needle lift and the radially eccentric location were set in terms of the micrometers reading before the water was emerged.

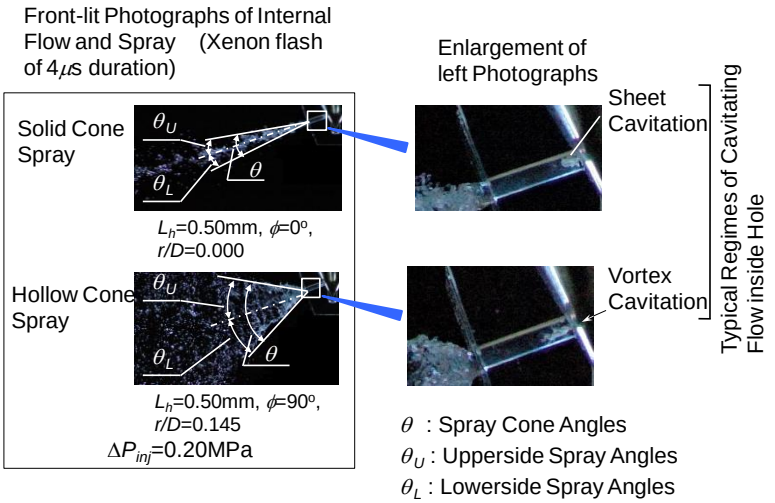

Figure 4 Typical shapes of spray and cavitating bubbles.

The large-scaled VCO nozzle had two nozzle holes with injection angle of 140° as illustrated in Fig. 3 (a). Both the holes had sharp-edged circular shape at the entrance of the holes. The diameter of both the nozzle holes was 2mm and the length was 8mm, providing a length to diameter ratio of 4. The large-scaled VCO nozzle was 10 times larger than real-size diesel nozzles. At an injection pressure of 0.20MPa the Reynolds number of the flow inside the hole of the large-scaled VCO nozzle was achieved at that of approximately 40000. The Reynolds number of the large-scaled VCO nozzle was nearly the same value as that of real-size diesel nozzles. The needle lift and the radial location denote L_h and r, respectively. ϕ describes the azimuthal angle from common plane of the two holes axes. However our coordinate system is different from conventional cylindrical coordinate system. Figures 3 (b) and (c) explain radial locations at the azimuthal angle of 0° and 90°, respectively. The radial location which has negative value is opposed to that which has positive value in our coordinate system. There exists the radial location along the direction of the nozzle holes at the azimuthal angle of 0° (Fig. 3 (b)). As the value of the radial location decreases at the azimuthal angle, the needle approaches the entrance of the nozzle hole for observation.

Optical system, which is illustrated in Fig. 1, was not employed as the spark photographs of sprays and cavitating bubbles were taken. Cavitating bubbles inside the nozzle and spray were illuminated simultaneously by two Xenon flashes of 4μs duration. Therefore front-lit photographs of cavitating bubbles and the spray were captured by a digital still camera as depicted in Fig. 4. Instantaneous behavior of the liquid jet breakup could be observed from each photograph, and spray cone angle θ, upperside spray angle and lowerside spray angle θ_L were estimated by using the photograph. Temporal behavior of cavitating bubbles were observed by using enlarged images of the spark photographs.

For the flow visualization inside the nozzle a halogen lamp with 450W which was incorporated into a slide projector was used as light source as illustrated in Fig. 1. Light originated from the projector passed through collimating lenses, and then the light was directed upward toward a nozzle hole, so that the tracer particles were illuminated. Photographs of stream lines of the tracer particles were captured by using a digital still camera. The shutter speed of the camera was 1/500 seconds in the flow visualization. In this work, fine powder of cross-linked poly methyl methacrylate with an average particle size of 50μm was used as tracer particles as shown in Table 1. The suspension was prepared by dispersing 1.6mg powder in every 1cc solution of water with surfactant.

Results and Discussion

Two typical breakup behaviors of liquid jets are obtained as demonstrate in Fig. 4: one is the behavior of "solid cone spray", and another is the behavior of "hollow cone spray". In contrast to the solid cone spray, many large droplets at the periphery of the hollow cone spray are yielded at the end of the conical liquid sheet. Regarding observation inside nozzle hole, two typical form of cavitating bubbles are observed inside the nozzle hole: one is yielded at upperside (and some times at lowerside) of the hole entrance. Another is produced along the centerline of nozzle hole and has a string-like shape. In this study, former is called "sheet cavitation", and latter is called "vortex cavitation". The vortex cavitation is usually accompanied by sheet cavitation as mentioned later.

Figure 5 illustrates the effect of the needle lift and the azimuthal angle on the spray cone angles [7]. At high needle lift of L_h=3.00mm the spray cone angle remains almost constant as the value of the radial location increases up to r/D=0.50. The spray cone angle are very sensitive to the radial locations of needles at low needle lift of L_h=0.50mm. At the low needle lift of L_h=0.50mm measuring range of the radial location is smaller than that for L_h=3.00mm due to extremely smaller needle lift. At the azimuthal angle of ϕ=0°, the spray cone angle increases with increasing the value of the radial location monotonically. In contrast to this case, the trend of the spray cone angle becomes very complicated at the azimuthal angle of ϕ=90°. Furthermore the spray cone angle in this case is larger than the angles in other cases. The significant increase of spray cone angle around the nozzle center and the complicated trend must be caused by a narrow gap between the needle and the seat because of lower needle lift and the eccentric location of the needle. This figure shows symmetry of both the profiles obtained at ϕ=90°, as opposed to the profiles obtained at ϕ=0°. Following discussion focuses on the behaviors at relatively low needle lift, and the needle is manipulated vertical to both the holes.

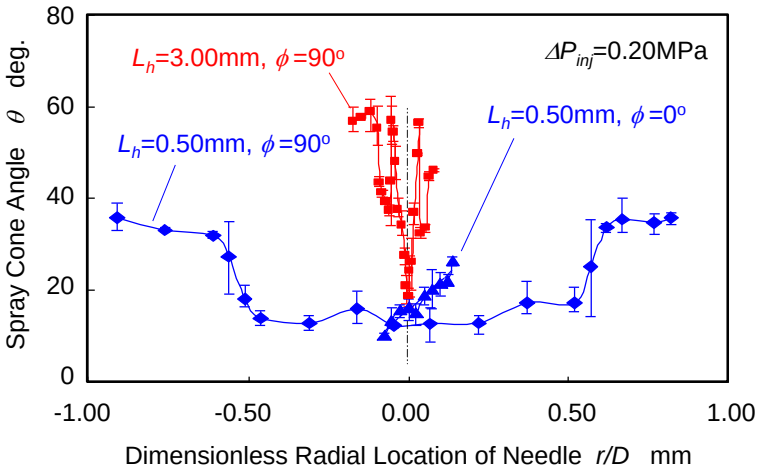

Figure 5 Effect of needle lift and azimuthal on spray cone angle.

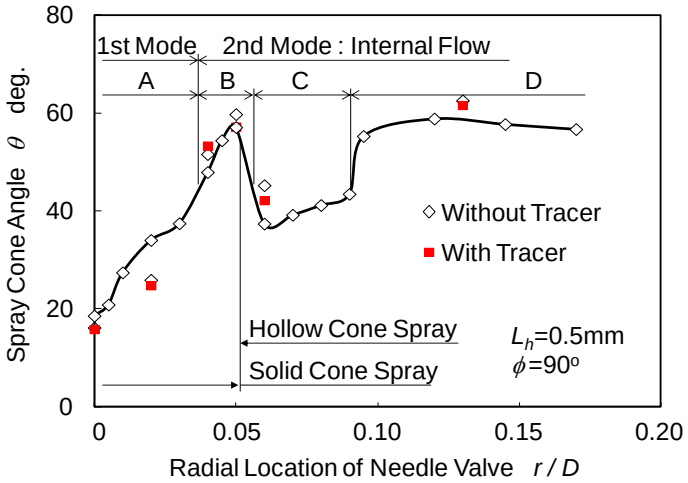

A: Upperside and Lowerside Sheet Cavitation
B: Upperside Sheet Cavitation and Partial Vortex Cavitation
C: Upperside Sheet Cavitation and Fully Covered Vortex Cavitation
D: Upperside Sheet Cavitation and Partial Vortex Cavitation

Figure 6 Effect of tracer particles on spray cone angle.

Open symbols appeared in Fig. 6 indicate results of spray cone angles without tracer particles [7]. The spray cone angle increases with the value of radial location of the needle among the regime A (Upperside and lowerside sheet cavitation in Fig. 7 (b)). In the regime A bubbles of sheet cavitation are apparent at upperside and lowerside of the entrance. These bubbles are produced by contractions. Regime B is the so-called transient regime (Upperside sheet cavitation and partial vortex cavitation in Fig. 7 (b)). Short bubble of the vortex cavitation is produced with the upperside bubble of sheet cavitation at the entrance of the hole while the lowerside bubbles can not be appeared any more. The solid cone spray or the hollow cone spray can be appeared in the regime B. And then the bubble of the vortex cavitation is elongated to the exit of the hole, so that the "air-core" is produced (Regime C: fully covered vortex cavitation in Fig. 7 (b)). Consequently, the spray cone angle reaches peak value, and the spray cone angle is significantly diminished as exhibited in Fig. 6. Finally, the bubble of the vortex cavitation becomes short as the needle is located enough far from a nozzle center in spite of relatively large spray cone angle (Regime D: partial vortex cavitation in Fig. 7 (b)). Thus two types of vortex cavitation bubbles, the string-like short bubble and the air-core, are observed.

It seems that the radially eccentric needle may promote contractions of main stream and reduction of static pressure at the hole entrance. Thus the reduction of the static pressure may lead to increase of gaseous volume produced by the upperside sheet cavitation in spite of disappearance of the lowerside bubbles. The string-like short bubble may cause to additional reduction of static pressure around the center of the hole in the regime B. Conical liquid sheet is yielded by the swirl motion, and ambient air may be pulled immediately into the hole on the transition from the regime B to the regime C. Hence, the air-core produced may come into contact with the

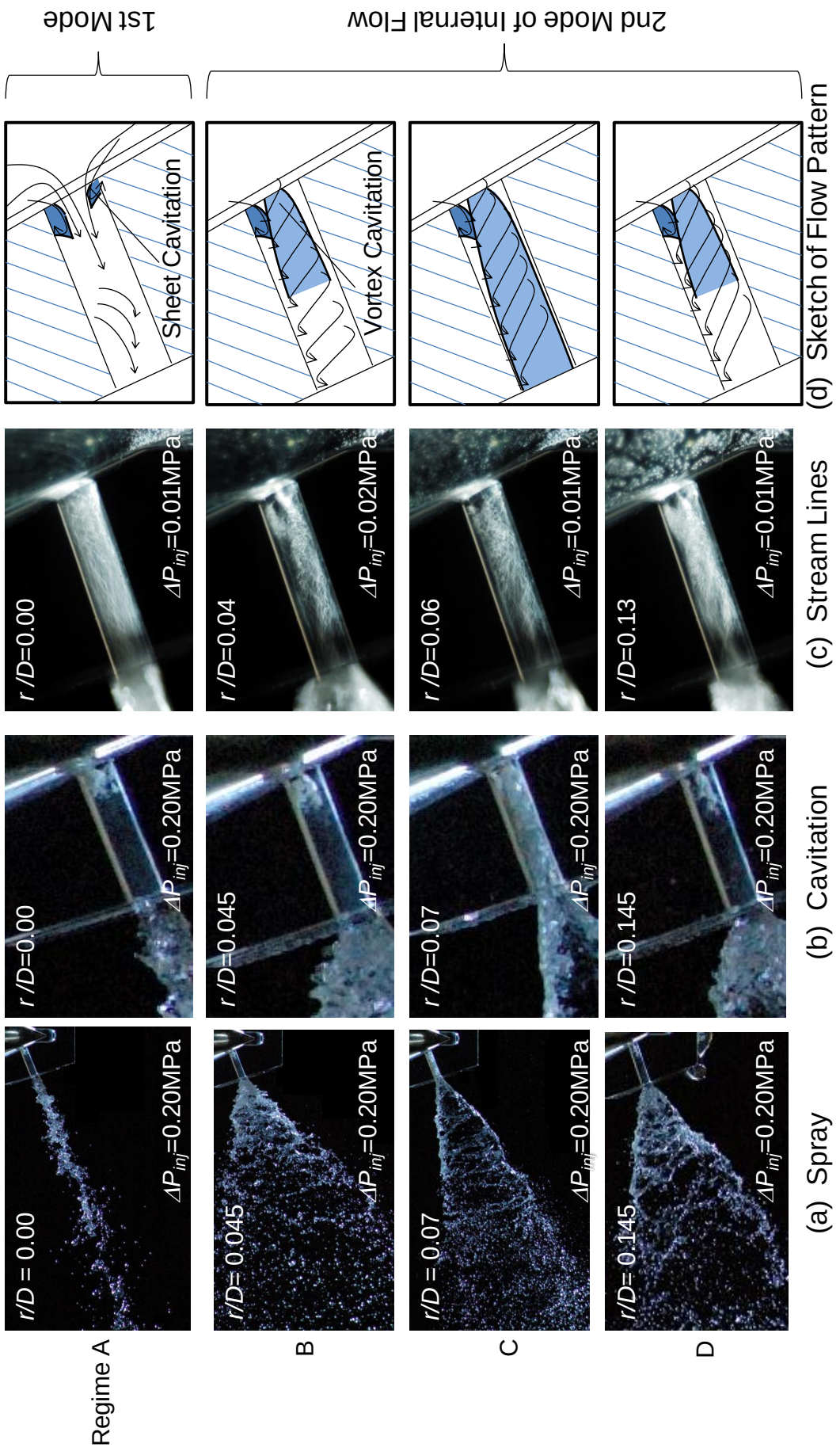

Figure 7. Effect of radial location of an eccentric needle on spray, cavitating and bubbles flow pattern. (ΔP_{inj} =0.20MPa, L_h=0.5mm, ϕ=90°)

string-like short bubble, and then the air-core reaches the hole entrance, and finally area of the upperside contraction and volume of the upperside bubble may decline.

The solid cone spray is observed when the needle is located near the center of the nozzle, and the hollow cone spray is apparent when the needle is located relatively far from the center of the nozzle as illustrated in Fig. 6. Solid symbols in Fig. 6 indicate results of spray cone angles with tracer particles. There is no significant difference between the spray cone angles with and without tracer particles.

Figures 8 (a), (b) and (c) show photographs of stream lines of tracer particles inside the hole at the radial location of r/d=0.04, and each photograph was obtained at different injection pressure. Figure 8 (d) exhibits the cavitating bubbles of the spark photography. Unfortunately, there is few information of flow pattern around the bubbles at the injection pressure of 0.20MPa (Fig. 9 (c)), which are produced at the hole entrance, because intensity of the scattered light of the particles is low, compared to the intensity of reflected light from the cavitating bubbles. However stream lines is observable at the downstream of the cavitating bubble and, fortunately, the flow pattern of the stream lines agree well with the flow patterns at the injection pressure of 0.01MPa and 0.05MPa (Figs. 9 (a) and (b), respectively). It is important to note that the injection pressure might hardly affect the flow patterns.

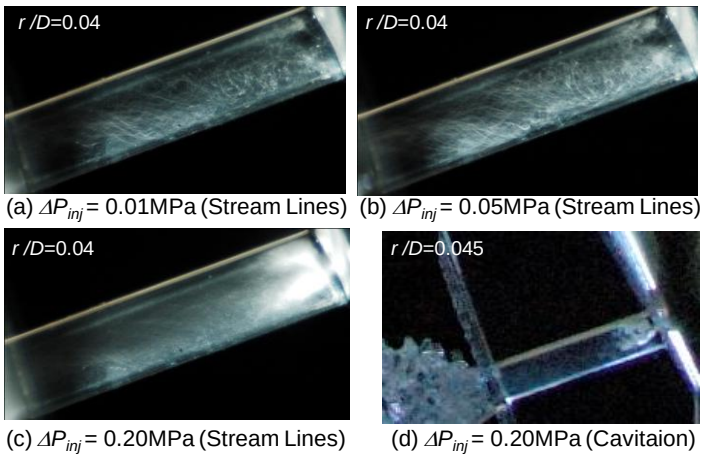

(a) ΔP_{inj} = 0.01MPa (Stream Lines) (b) ΔP_{inj} = 0.05MPa (Stream Lines)

(c) ΔP_{inj} = 0.20MPa (Stream Lines) (d) ΔP_{inj} = 0.20MPa (Cavitaion)

Figure 8 Effect of injection pressure on flow pattern. (ΔP_{inj} =0.20MPa, L_h=0.5mm, ϕ =90°)

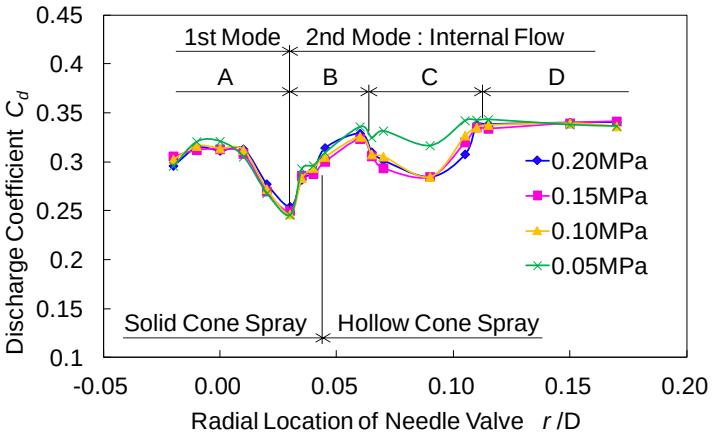

A: Upperside and Lowerside Sheet Cavitation
B: Upperside Sheet Cavitation and Partial Vortex Cavitation
C: Upperside Sheet Cavitation and Fully Covered Vortex Cavitation
D: Upperside Sheet Cavitation and Partial Vortex Cavitation

Figure 9 Effect of injection pressure on discharge coefficient. (L_h=0.5mm, ϕ =90°)

Figure 9 represents the effect of injection pressure on the discharge coefficient [8]. It is interesting to see from this figure that the radial locations of the regimes A, B, C and D hardly depend on the injection pressure and the value of the discharge coefficient is less dependent on the injection pressure. These results suggest that the injection pressure hardly influences flow pattern inside the nozzle and that the ratio of the angular momentum to axial momentum of ejecting liquid induced by the eccentricity may dominate flow pattern inside the nozzle and structure of the spray strongly.

The swirl angle is defined as the angle between a centerline of the hole and a stream line across the center line as shown in Fig. 10. It is reasonable to suggest that the swirl angle is identical to a ratio of an angular momentum of the swirl motion to an axial momentum. Two swirl angles of liquid flow inside the hole are estimated from the photographs of stream lines: one was a midpoint swirl angle $\theta_{S,M}$ which is measured at the midpoint between the entrance and the exit of the hole, and another is an exit swirl angle $\theta_{S,E}$ at the exit of the hole. Figure 11 exhibits the effects of the injection pressure on swirl angles. The midpoint swirl angle and the outlet swirl angle show similar trends to the spray cone angle in the regimes A, B and C as follows. The swirl angles increase with increasing the value of the radial location up to r/D=0.05, and then the swirl angles are diminished significantly. Further increase, the swirl angles reach almost constant value. Value of the exit swirl angle is similar to that of the midpoint swirl angle in the regimes B and C while there is difference between the exit swirl angle and the midpoint swirl angle in the regime A. It is remarkable that both the swirl angles are independent

of the injection pressure and that the radial location of needle influences the swirl angles in the same way as the discharge coefficient as illustrated in Fig. 9.

Sketches of flow patterns as illustrated in Fig. 7 (d) are obtained from the photographs of stream lines (Fig. 7 (c)). As the needle is located at the radial location of r/D=0, undisturbed straight stream lines along the hole are apparent at the downstream of the midpoint while disturbed stream lines are observed near the hole entrance. Contraction regions are produced at upperside and lowerside of the hole entrance. High injection pressure lead to cavitating bubbles at these contraction regions. If the eccentric needle is located close to the nozzle center, main stream has weak vortex motion. Additionally, both the contraction regions remain at the hole entrance concerning the regime A.

On the contrary to first mode of flow pattern described above, visualization shows another mode of flow pattern, second mode, in the regimes B, C and D. Strong vortex motion along the hole from the entrance to the exit is induced by the eccentric needle. The inspection of flow pattern shows a "pocket-like" region, which is located at upperside of the hole entrance, and contracted main stream passes below the "pocket-like" region while lower contraction is disappeared. Although similar flow pattern is obtained in the regimes B, C and D, two different types of vortex cavitating bubbles are appeared as mentioned above.

Figure 12 represents the effect of the radial location of the needle on upperside and lowerside spray angles. Trends of the upperside spray angle and the lowerside spray angle are almost the same as that of the spray cone angle which is illustrated in Fig. 6. There are no significant differences between values of the upperside spray angle and of the lowerside spray angle in the regimes A and C. In contrast, the distinct differences can be appeared in the regimes B and D. The contracted main stream below the "pocket- like" region expands upwardly, so that the main stream reaches upperside of the hole at the downstream of the "pocket- like" region. This result suggests that the relatively upward stream might lead to increase the upperside spray angle in the regime B and D. It must be emphasized here that the flow pattern and the swirl motion greatly influences the spray angles. In other words behavior of the primary atomization corresponds to the flow pattern inside the hole.

Conclusions

Flow visualization was carried out to clarify the effects of eccentricity of a needle inside a valve-covered-orifice (VCO) diesel nozzle on structure of internal flow. The visualization shows that flow pattern strongly depend on radially eccentric location of the needle. On the contrary the flow pattern is almost independent of injection pressure. Several conclusions are as follows:

(1) Flow visualization for first mode of internal flow indicates almost straight stream with weak swirl motion inside the hole when the eccentric needle is located close to the nozzle center. The flow pattern of the first mode leads to the solid cone spray. High injection pressure leads to cavitating bubbles at upper side and lower side contraction regions, which are produced at the entrance of the hole.

(2) Another mode, the second mode of internal flow, is encountered when distance of the needle from the nozzle center is further increased beyond the radial location of the first mode. The flow pattern of the second

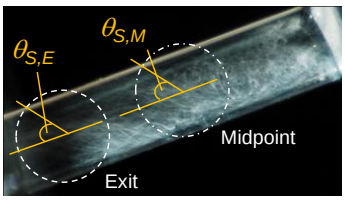

Figure 10 Definition of swirl angle. (ΔP_{inj}=0.20MPa, L_h=0.5mm, ϕ=90°)

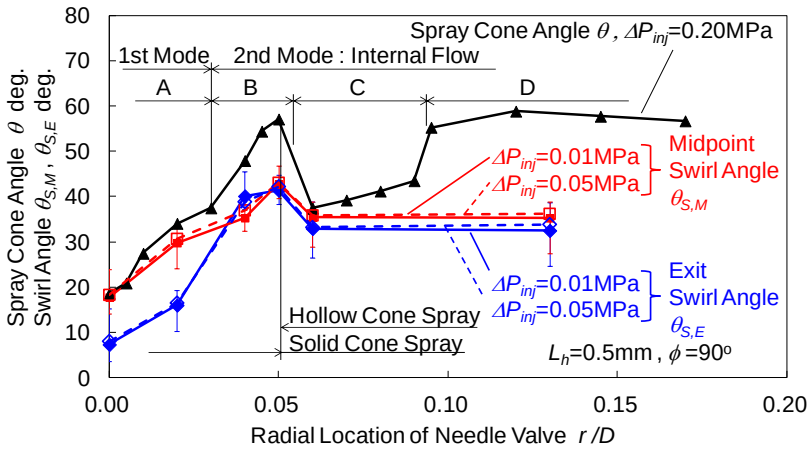

A: Upperside and Lowerside Sheet Cavitation
B: Upperside Sheet Cavitation and Partial Vortex Cavitation
C: Upperside Sheet Cavitation and Fully Covered Vortex Cavitation
D: Upperside Sheet Cavitation and Partial Vortex Cavitation

Figure 11 Effect of radial location of an eccentric needle on spray cone angle and swirl angle.

mode shows strong swirl motion, so that the hollow cone spray is mainly appeared. High injection pressure leads to producing bubble of the vortex cavitation. The contraction region at the upperside of the entrance remains although the lowerside contraction region at the hole entrance becomes undetectable.

(3) The spray cone angle is related to the swirl angle of swirl motion along a hole, which was obtained by using the photograph of the stream line inside the hole.

(4) The contraction regions affect the upperside and lowerside spray angle.

References

[1] Renner, G, Koyanagi, K. and Maly, R. R., *Proc. the Fourth International Symposium on Diagnostics and Modeling of Combustion in internal Combustion Engines (COMODIA 98)*: pp. 477-482 (1998).

[2] Fettes, C., Heimgärtner, C. and Leipertz, A., *The Fifth International Symposium on Diagnostics and Modeling of Combustion in Internal Combustion Engines (COMODIA 2001)*: pp.54-59 (2001).

[3] Tsunemoto, H., Ishitani, H., Montajir, R., Hayashi, T., Kitayama, N., *The Fifth International Symposium on Diagnostics and Modeling of Combustion in Internal Combustion Engines (COMODIA 2001)*: pp.528-533 (2001).

[4] Kim, J. H., *Ph. D. Thesis*, University of Hiroshima: (2001) (in Japanese).

[5] Liverani, L., Arcoumanis, C., Yanagihara, H., Sakata, I. and Omae, K., *Proc. Seventh COMODIA International Symposium on Diagnostics and Modeling of Combustion in internal Combustion Engines*, JSME No.08-202: pp. 453-460.

[6] Kim, J. H. Nishida, K. and Hiroyasu H., *The 7th Internal Conference on Liquid Atomization and Spray Systems (ICLASS-'97) Proc.*: pp. 175-182 (1997).

[7] T. Oda, S. Kanaike, K. Aoki, Y. Goda and K. Ohsawa, *Proc. Of the 12th Annual Conference of ILASS-Asia and the 17th Symposium (ILASS Japan) on Atomization*: pp.21-26 (2008).

[8] T. Oda, Y. Goda, S. Kanaike, K. Aoki and K. Ohsawa, *Proceedings of the 11th Triennial International Annual Conference on Liquid Atomization and Spray Systems*, paper number 132: (2009).

[9] T. Oda, M. Hiratsuka, Y. Goda, S. Kanaike and K. Ohsawa, *23rd Annual Conference on Liquid Atomization and Spray Systems-Europe*, 72: (2010).

[10] K. Kitamura, M. Hiratsuka, K. Ohsawa, T. Oda and T. Sumi, *Proc. of the 22nd Internal Combustion Engine Symposium Japan*: pp. 219-224 (2011) (in Japanese).

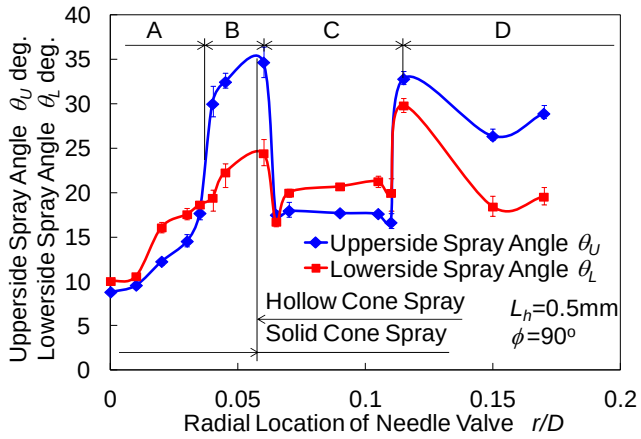

A: Upperside and Lowerside Sheet Cavitation
B: Upperside Sheet Cavitation and Partial Vortex Cavitation
C: Upperside Sheet Cavitation and Fully Covered Vortex Cavitation
D: Upperside Sheet Cavitation and Partial Vortex Cavitation

Figure 12 Effect of radial location of an eccentric needle on upperside and lowerside spray angle. (ΔP_{inj} =0.20MPa)